Liquid ^{4}He: an ordinary and exotic liquid

1996 J. Phys.: Condens. Matter 8 9249

(http://iopscience.iop.org/0953-8984/8/47/012)

J. Phys.: Condens. Matter **8** (1996) 9249–9262. Printed in the UK

Liquid ^{4}He: an ordinary and exotic liquid

A F G Wyatt

Department of Physics, University of Exeter, Stocker Road, Exeter, Devon, UK

Received 15 July 1996

Abstract. Liquid ^{4}He is a unique liquid because of its Bose nature but it can be used to study general problems. A number of such properties are reviewed including quantum evaporation, interactions between excitations and wetting studies with Cs.

1. Introduction

Liquid ^{4}He is well known for its extraordinary superfluid properties. However it is also an important liquid for studying some general properties of liquids and phonons. In this brief review we shall illustrate this latter aspect with examples such as four-phonon scattering and wetting studies which are best done using liquid ^{4}He, as well as describing some phenomena which are unique to ^{4}He such as quantum evaporation and the creation of beams of ballistic excitations.

2. Background

Liquid ^{4}He is the simplest liquid that exists as the atoms are spherically symmetric and only weakly interact via the van der Waals potential. There is a good chance that eventually it will be understood completely but that point is a long way off as liquid ^{4}He is a complicated many-body system. However, many of the basic properties starting from the interatomic potentials of helium are already understood.

The most significant point about liquid helium is that is remains a liquid down to $T = 0$ K, see figure 1. It is this fact that allows the quantum nature to become obvious and is in contrast to all other liquids which turn into solids before the effect of quantum statistics becomes significantly different to classical statistics. The quantum nature of liquid ^{4}He is spectacularly different to other liquids as it is superfluid, and exhibits quantum coherence on a macroscopic scale. This gives its vortices quantized circulation and makes it possible for the liquid to show the Josephson effect. Equally remarkable is the fact that liquid ^{4}He has extremely well defined elementary excitations. These are delocalized and account for the dynamic and thermodynamic properties of the liquid.

^{4}He is a boson whereas ^{3}He is a fermion. The two liquids have approximately similar phase diagrams where the interatomic potentials play the dominant role. However the ground states of the two liquids are quite different reflecting the difference between the two types of statistics. Liquid ^{4}He has a superfluid transition temperature at 2.17 K while for liquid ^{3}He it is at 2 mK. Furthermore the excitations in liquid ^{3}He have a short lifetime in contrast to the infinite lifetime for some of the excitations in ^{4}He.

0953-8984/96/479249+14$19.50

The thermal de Broglie wavelength $\lambda_{th} = h(3mkT)^{-1/2}$ for a gas of atoms with mass m at temperature T can be longer for helium than for any other substance as m is small and T can be reduced towards zero. At 1 K, λ_{th} is four times larger than the interatomic spacing in liquid helium. This indicates that we should expect the atoms in liquid helium to be much more strongly correlated than in other liquids where λ_{th} is much less than the atomic or molecular spacing, in which case the particle-like properties of the atoms or molecules are dominant.

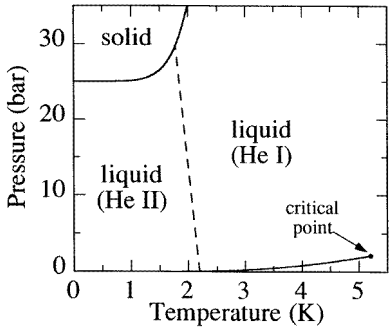

Figure 1. The phase diagram for ^{4}He: the dashed line is the superfluid–normal transition.

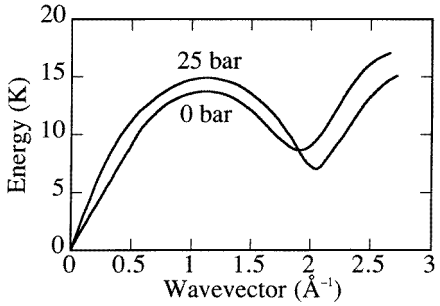

Figure 2. The dispersion curve for the excitations of liquid ^{4}He.

The excitations in liquid helium are indeed due to collective motions of many atoms and are certainly very different to other liquids. The excitations in liquid ^{3}He and ^{4}He are quite distinct, due to the different statistics, and we shall only discuss liquid ^{4}He from now on. The dispersion curve of the excitations can be measured by neutron scattering to great precision [1]; $\omega(q)$ is shown in figure 2. At low wavevectors the excitations are phonons with nearly linear dispersion and there are no excitations that are anything like free particles [2]. At higher wavevectors the phonon-like behaviour disappears and the dispersion curve has a minimum where the excitations are called rotons. This is an unfortunately confusing name because there is no angular momentum associated with a roton [3]. The rotons to the left and right of the minimum are called R^- and R^+ rotons respectively due to their negative and positive group velocities with respect to their momenta.

The dispersion curve can be derived theoretically starting from the interatomic potentials, the latest calculations [4] get results quite close to the measured values. However, whereas we can easily picture the phonon excitations we still do not have a detailed description of a

roton. The working hypothesis is that it is a moving helium atom surrounded by a backflow of helium liquid [2, 5]; at the roton minimum the mass current is zero due to equal and opposite contributions from the atom and backflow. On the low-q side of the minimum the backflow contribution dominates and on the high-q side, the atom contribution dominates the roton's momentum.

The number of thermally excited phonons and rotons varies rapidly with temperature. For $0 < T < 0.6$ K there are essentially only phonons as the energy gap for rotons, $\Delta = 8.6$ K, is so large compared to T. At $T \sim 1.2$ K there are equal numbers of phonons and rotons but most of the energy is in the rotons, and for $T > 1.2$ K the roton density dominates. As T is reduced below 0.6 K the number of phonons decreases as T^3 so by going to lower temperatures the number of thermal excitations can be reduced to arbitrarily low values. This gives the excitation model of liquid ^{4}He. There is the ground state which is the liquid at $T = 0$ K, and at finite temperatures there is the ground state plus excitations [2]. The excitations do not interact strongly if their density is not too high, so the excitation model applies for $T \leqslant 1.5$ K.

The fact that we can reduce the number of thermally excited excitations to essentially zero means that if excitations are created by a small source then they travel ballistically away from the source. This allows beams of phonons and rotons to be made which are not scattered significantly by thermal excitations for $T < 0.1$ K over paths $\leqslant 1$ cm.

However some excitations spontaneously decay. A phonon with energy $\omega < 8$ K decays to two phonons by the three-phonon process (3pp) and for $8 < \omega < 10$ K a phonon decays into three or more phonons [6, 7]. The lifetime against spontaneous decay varies as $\sim \omega^{-5}$ for the 3pp and phonons with $\omega \sim 8$ K only travel $\sim 10^2$ nm before decaying [8]. Phonons with $\omega > 10$ K cannot spontaneously decay so at low temperatures they have essentially infinite lifetimes. The change in lifetime is discontinuous at $\omega_c = 10$ K.

Phonons behave this way in liquid ^{4}He at zero pressure because the upward dispersion of $\omega(q)$ allows energy and momentum to be conserved in a spontaneous decay process. For higher pressures the region of upward dispersion becomes less and ω_c decreases with pressure [9], going to zero at 19 bar [10, 11]. For pressures $19 < P < 25$ bar all phonons are stable against spontaneous decay. It is worth noting that the large compressibility of liquid ^{4}He, which causes the phonon velocity to increase from 238 ms^{-1} to 361 ms^{-1}, is due to the large zero-point motion of the atoms at $P = 0$ which can be reduced by pressure.

Most and perhaps all rotons are stable against spontaneous decay. If there is a decay it would be a roton scattering to another roton and a small phonon i.e. $R \rightarrow R' + p$ [12]. This will only happen if the roton group velocity exceeds the phonon velocity at low ω. The highest group velocity of rotons occurs at the inflection point in $\omega(q)$ at $q \sim 2.3$ Å^{-1}, but the neutron data is not sufficiently accurate to resolve this question. From experiments on ballistic rotons [13] it appears that any region of $\omega(q)$ where $v_g > v_p$ is small, $\delta q < 0.1$ Å^{-1}. At pressures > 0 the phonon velocity rises but the roton group velocity is essentially unchanged, so it is then clear that all rotons are stable against spontaneous decay.

We have now reviewed the essential properties of liquid ^{4}He so that we can discuss the work on ballistic beams of excitations. This will give a much more detailed understanding of the excitations and their interactions.

3. Quantum evaporation

If a beam of phonons or rotons is directed at the free surface of liquid ^{4}He there are, in principle, a number of possible outcomes. For example it might reflect, mode change to

another excitation species, create a ripplon or knock out an atom from the liquid state into the vacuum state. Higher-order processes would combine these possibilities. To evaporate an atom the excitation must have enough energy to overcome the binding of the atom to the liquid. In liquid ^{4}He this is $E_B = 7.16$ K and from figure 2 it is clear that there are high frequency (hf) phonons and all the rotons with enough energy. In a one-to-one process where the phonon or roton is annihilated at the surface, the excess energy appears as kinetic energy of the atom,

$$\hbar\omega = E_B + p^2/2m_4. \tag{1}$$

Equation (1) has been verified in a number of experiments using time of flight measurements and is now well established.

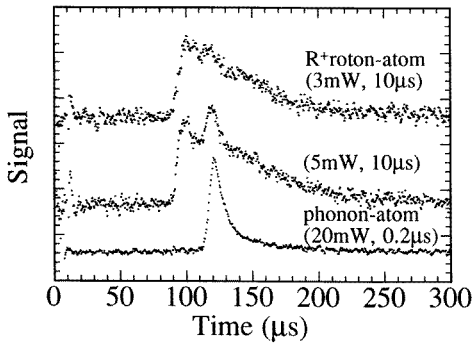

Figure 3. Examples of quantum evaporation signals. The middle curve shows evaporation by both phonons and rotons. Note that the R^+ roton–atom signal is much more dispersed than the phonon–atom one.

Some example signals of quantum evaporation (QE) are shown in figure 3. The excitations are produced by pulse heating a thin metal film immersed in the liquid ^{4}He and the atoms are detected by the energy that they give when they condense onto a bolometer. It is possible to create either mainly hf phonons or mainly rotons by varying the energy and duration of the pulse to the heater, because the creation processes are quite different for these excitations. We shall discuss this later.

In figure 3 it is apparent that the roton–atom signal is much broader in time than the phonon–atom signal. This is due to the hf phonons having a narrow spectrum around $\omega \sim 10$ K while the rotons have a wide group velocity spectrum which ranges from zero at the minimum in $\omega(q)$ to the maximum at the point of inflection. The overall signal time of course depends on the atom's velocity too, so the energy of the excitation, as well as its velocity, is important. The large dispersion of the roton–atom signal means that roton spectroscopy is possible as the signal at any instant relates to a narrow range of roton energies.

If the beam of excitations is directed at the surface at a finite angle of incidence then the translational symmetry of the surface requires that the component of momentum parallel to the surface is conserved. This gives a strong refraction effect which is illustrated in figure 4. A beam of mixed excitations, at the same angle of incidence, evaporate atoms into three angular sectors. R^+ rotons have most momentum so the quantum evaporated atoms are at large angles to the normal. Phonons have the smallest momentum and create an atom beam closer to the normal than the angle of incidence. R^- rotons have a negative

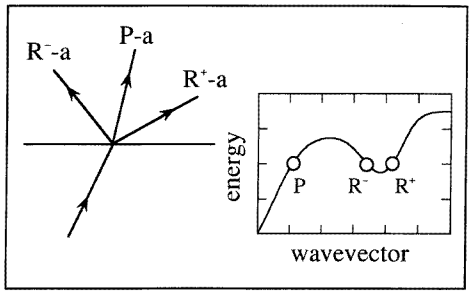

Figure 4. Schematic diagram of the refraction in quantum evaporation by phonons, P, R^+ rotons and R^- rotons. The inset shows these excitations on the dispersion curve.

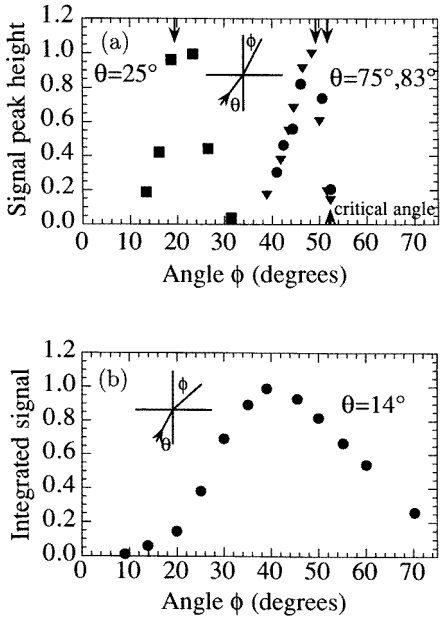

Figure 5. (a) Three examples of phonon–atom quantum evaporation. The data are the angular distribution of atoms from phonons with incident angles 25°, 75° and 83°. The arrows at the top show the calculated angles for 10.5 K phonons for these angles of incidence. The arrow at the bottom indicates the critical angle for 10.5 K phonons: this is the maximum angle for evaporated atoms for this energy. (b) The angular distribution of atoms evaporated by R^+ rotons at an angle of incidence of 14°. The angular distribution is much wider than for phonons due to the relatively large range of roton energies.

group velocity so if the group velocity is towards the surface then the momentum is in the opposite direction and the atoms are evaporated into the opposite quadrant to the atoms from the other two types of excitation. The atoms from hf phonons and R^+ rotons have been detected [13] and are shown in figure 5(a) and (b) respectively, and the refraction angles are consistent with $q_\parallel = k_\parallel$ where q and k are the wavevectors of the excitation and atom respectively.

The angular experiments show that the atoms which are evaporated do not have any additional momentum over that from the excitation and the recoil of the liquid as a whole. This indicates that the atoms are being quantum evaporated from the $k = 0$ state. However atoms in the liquid have a considerable expectation of a non-zero momentum, even in the ground state, which can be measured by neutron scattering [14] and is due to the confinement of each atom by other atoms. The evaporated atoms are also not scattered which indicates that they come from the outer region of the density profile at the surface. Here the atoms are less confined than in the bulk liquid and so have a greater probability of $k = 0$.

No atoms due to R^- rotons have been clearly detected and this presumably is either due to R^- rotons not being created by the heater or because the probability of QE is very small for these rotons. We are inclined to think that the former reason is why we have not seen them. R^- rotons have been created using a spongy heater which acts more like a black-body source [15]. However this source is slow and cannot be used for time of flight measurements which would confirm the R^- roton–atom process, so we need to develop a fast black-body source for R^- rotons.

The opposite process to QE is condensation. An atom beam is directed at the free surface of liquid ^{4}He and a bolometer in the liquid is scanned in angle. The result is shown in figure 6 [16]. There is a relatively large signal where R^+ rotons are expected. It is not clear whether this is due to the direct detection of rotons or low-energy phonons from roton–phonon scattering. This uncertainty arises because rotons have not been detected in direct propagation from a heater to a bolometer in the liquid. However in such an arrangement a roton beam is always accompanied by low-energy phonons which probably have a flux two orders of magnitude higher in energy and so may mask the rotons even though they are dispersed in time from the phonons.

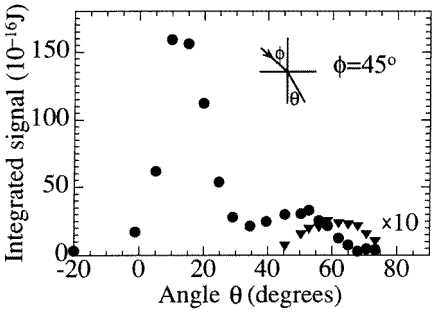

Figure 6. The angular distribution of excitations in the liquid ^{4}He due to condensing atoms at 45° angle of incidence. The main peak is at the R^+ roton angle, the secondary peak is due to the creation of two phonons at the surface, and the minor peak (triangles) is due to the creation of one phonon per atom.

The condensation process shows a very weak signal due to the one-to-one creation of hf phonons, and a new process where an atom creates two or more phonons at the surface. Recent experiments [17] show that condensing atoms are most likely to create ripplons. As ripplons have a large momentum relative to their energy, compared to an atom, they must be created in pairs or higher numbers.

The theory of quantum evaporation has proved to be a difficult challenge. It is necessary to calculate how the excitations change in the surface region from their bulk-liquid character [18, 19]. Recently there have been calculations of the probability of the various one-to-one processes involving rotons and atoms [20]. This in turn has posed a challenge to measure

these probabilities which is difficult because there is no way of measuring the roton flux. The situation is somewhat better for hf phonons as the flux can be estimated, and it is found that the probability of a phonon evaporating an atom is ~ 0.1 [21].

All these experiments described above indicate that quantum evaporation is the analogue of the photo-electric effect. Not only do they show that there are one-to-one processes that conserve energy and parallel momentum, they provide a way for hf phonons and R^+ rotons to be detected and distinguished from each other and from low-energy phonons. This enables a series of experiments to be performed on these excitations which would otherwise be impossible. We shall now discuss these scattering experiments and the generation of high-energy excitations.

4. Four-phonon scattering

As we explained in section 2, a hf phonon, i.e. one with $\omega > 10$ K, does not spontaneously decay so it is only scattered in a collision with another excitation. At low temperatures, $T < 0.6$ K, the most important scattering is with thermal phonons in a four-phonon process (4pp), i.e. $P + p \rightarrow P' + p'$ where P is the hf phonon and p is the thermal phonon. These phonons are annihilated and the P′ and p′ phonons created. P′ can have momentum in the range $\frac{1}{2}|\boldsymbol{P} + \boldsymbol{p}| \leqslant |\boldsymbol{P}'| \leqslant |\boldsymbol{P} + \boldsymbol{p}|$. Liquid ^{4}He provides a unique opportunity to study the 4 pp in the absence of the 3pp, which if present as it is in solids, is dominant.

The scattering of hf phonons can be readily measured by the attenuation of a ballistic beam of hf phonons as it propagates through liquid ^{4}He at different temperatures. The hf phonons that reach the surface of the liquid are detected by QE. A hf phonon that is scattered almost certainly will not have enough energy to evaporate an atom because the energy of the larger created phonon, P′, is most likely to have $\omega < \omega_c$, which means it will rapidly decay by spontaneous processes to energies well below the atom's binding energy. So the situation is quite clear: only those hf phonons which have not been scattered contribute to the QE signal.

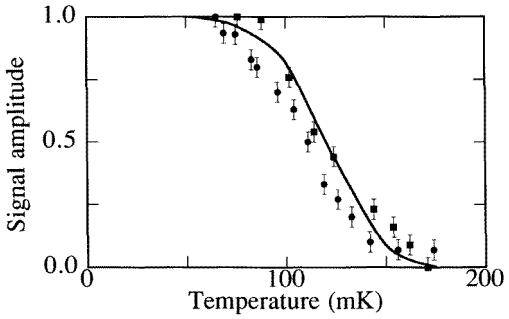

Figure 7. The attenuation of high-frequency phonons by thermal phonons. The circles are for high-frequency phonons detected in the liquid and the squares are for phonon–atom signals; path length is 15.7 mm. The solid line is calculated. All are normalized to unity at the lowest temperature.

The temperature of the liquid ^{4}He determines the density and spectrum of the low-energy phonons. As their density rises rapidly as T^3 we should expect that the hf phonon signal to rapidly attenuate at the temperature where the mean free path of the phonon is the same as the propagation distance through the liquid. This behaviour can be seen in figure 7, where

the QE signal drops rapidly at around $T \sim 0.12$ K for a propagation distance of 15.7 mm [22].

The hf phonon flux attenuates according to

$$\phi = \phi_0 \exp(-n\sigma d) \tag{2}$$

where n is the density of thermal phonons, σ is the 4pp scattering cross-section and d is the propagation distance. It is usual to give the scattering rate $\Gamma = v_g n\sigma$ where v_g is the group velocity of the hf phonons. Γ is shown as a function of T in figure 8 [23].

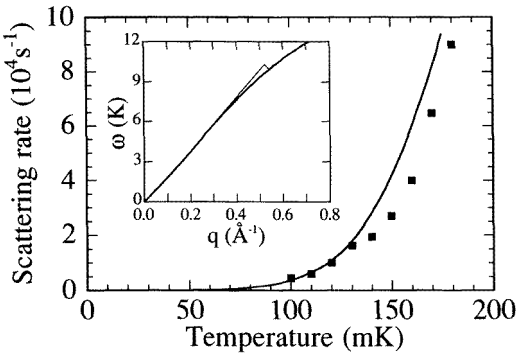

Figure 8. The measured data, squares, and the theoretical scattering rate of high-frequency phonons by the four-phonon process. The inset shows a high-frequency phonon and a thermal phonon scattering to produced two medium-energy phonons.

The theory of the 4pp in liquid ^{4}He was first published by Landau and Khalatnikov [24]. The principle of the interaction is that the low-frequency (lf) phonon modulates the density of the liquid and this perturbs the energy of the hf phonon. The matrix element is then used in Fermi's golden rule. The original theory gave a very strong interaction, so strong that ballistic progation at $T = 0.1$ K would be impossible. The theory was re-examined [22] and it was discovered that further diagrams, which had previously been neglected, were very important. There is a major cancellation between the original and new terms in the matrix element which makes the scattering $\sim 10^3$ smaller. This development completely changed the picture of the dominant scattering process. Originally it was thought that the created phonon P$'$ had a slightly higher momentum than the incoming phonon P. However the new terms show that the incoming phonon is down-converted, so P$'$ is likely to be much smaller than P. This process is shown inset in figure 8. The reason why this is the dominant process is that there is a much larger density of final states for down-conversion than for up-conversion.

The new theory agrees with the measurements as can be seen in figure 8. This is the first time that the 4pp process has been measured and described in detail by theory for any material.

The scattering rate is put into a larger context in figure 9 [25], where $\Gamma(T)$ is shown over a wide temperature range. At $T > 1.2$ K, hf phonons are scattered by thermal rotons and the scattering rate is five orders of magnitude higher than at 0.15 K. The high scattering rate causes a broadening of the phonon linewidth in neutron scattering measurements [26]. At $T < 1$ K the linewidths are too small to measure this way so there is a large range of temperatures where there is no technique available to measure the scattering rates. Also

included in figure 9 are the roton scattering rates which, on the logarithmic scale, are similar to the hf phonon rates.

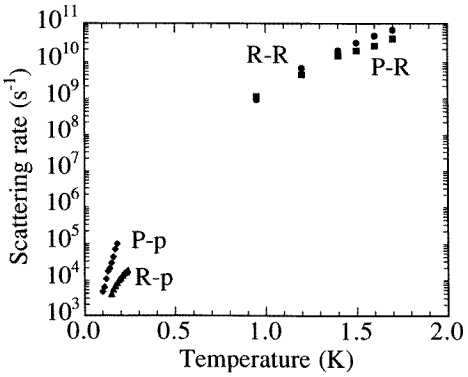

Figure 9. The scattering rates for high-frequency phonons and rotons with thermal excitations. The dominant scattering excitations are indicated by the second letter.

5. Roton–roton scattering

As we can create and detect ballistic roton beams, we have the possibility of studying interacting beams. In contrast to the phonon scattering described above, the beams are created in liquid ^{4}He at low enough temperatures so that there is a negligible number of thermal excitations. Using colliding beams means that in principle the scattering strength can be found as a function of energy and angle. We describe below the first such measurement. Roton–roton scattering can be inferred from macroscopic parameters such as viscosity, but this only gives a thermal average over rotons near the minimum in $\omega(q)$. With ballistic beams we can use time of flight spectroscopy and cover the wavevector spectrum from near the minimum to the point of inflection.

The experimental arrangement has one roton beam directed towards the free surface so that its flux, ϕ, can be monitored by QE. This is called the probe beam. The second beam is directed to intersect the probe beam and is called the scattering beam. The attenuation of the probe beam is given by equation (2) but now n is the density due to the scattering beam and d is the distance the probe beam propagates through the scattering beam. An example of the attenuated probe beam is shown in figure 10.

The sources of the roton beams are pulsed so rotons are time dispersed when they reach the interaction volume. The scattering is then predominantly between rotons of defined momenta. The applicability of equation (2) is checked by varying the number density of the scattering rotons. This can be done by either changing the heater pulse power or pulse length. Within the correct limits, the number density is a linear function of these parameters and it is found that the detected probe flux varies exponentially with n according to equation (2) [27].

The attenuation of the probe pulse is time, and hence roton-energy, dependent. To examine this in detail the timing between the pulses is arranged so that the probe rotons are interacting with slow scattering rotons. This gives a well defined set of scattering rotons which is not changing significantly on the time scale of the probe rotons tranversing it. The attenuated probe signal is compared with the unscattered probe signal at a set of points along

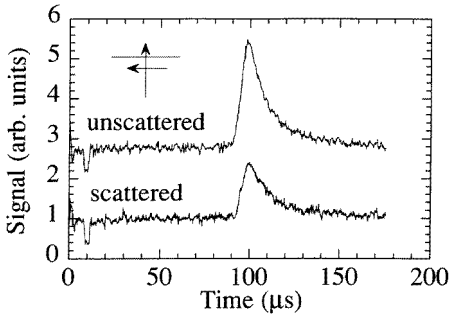

Figure 10. The unscattered R^+ roton–atom signal and when it is attenuated by scattering with a second R^+ roton beam.

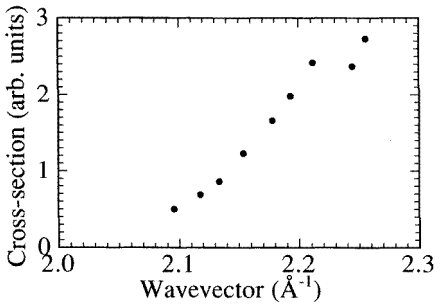

Figure 11. The R^+ roton–R^+ roton scattering cross-section as a function of wavevector of the probe roton.

the time axis. These times are related to the momenta of the probe rotons via equation (1) and the group velocity $v_g(q)$ from $\omega(q)$. The results are shown in figure 11 [28].

The results show that the scattering cross-section is strongly dependent on wavevector. σ changes by a factor of five between $q = 2$ Å^{-1} and $q = 2.25$ Å^{-1}. This was a surprising result and prompted theories to explain it. Iwamoto [29] suggested a resonant scattering between the two rotons, and Pitaevskii [30] considered the process $R + R \rightarrow R + R + P$ which he showed increased σ with q.

The vertical scale in figure 11 is the relative scattering cross-section σ. It cannot be calculated absolutely because there is no way of measuring the scattering roton density n. If we assume that 1% of the pulse energy into the heater goes to creating rotons then the scattering cross-section agrees to within an order of magnitude with other estimates from viscosity, roton second sound and neutron linewidth [27].

Although the scattering roton density is not known, the same density can be probed with hf phonons instead of rotons. Hence the ratio of roton–roton scattering to hf phonon–roton scattering can be obtained and compared to the ratio found from neutron scattering. As the scattering rate $\Gamma = n\sigma v_g$, we compare probe phonons and rotons with the same group velocity. Then $\Gamma_{PR}/\Gamma_{RR} = \sigma_{PR}/\sigma_{RR}$ and, as $\sigma \propto \ln(\phi_0/\phi)$, the ratio of the scattering rates can be found without any unknown quantities. The value of the roton group velocity, chosen to match the hf phonon group velocity, means that the high values of σ_{RR} near the resonance are avoided. The ratio of the scattering rates measured by neutrons agree with those from the QE measurements which is pleasing for such diverse techniques [31].

6. The creation of high-frequency phonons

The hf phonons and rotons used in QE experiments are created by a thin-film heater in the liquid ^{4}He. It had been assumed that these excitations were created at the heater–liquid interface and propagated ballistically away from this interface. This simple picture is neither right for rotons nor hf phonons. R^+ rotons are most likely created at the interface but there is a small region of scattering in front of the heater before they become ballistic. We explain below that hf phonons are not created at the heater surface and how this resolves a long-standing discrepancy between the measured and calculated arrival times for the phonon–atom signals.

The measured phonon–atom arrival time is $\sim 5\%$ faster than that calculated. This is outside experimental errors in either the group velocity from $\omega(q)$ or the measured time of flight. While it is not difficult to think of processes that would make the measured time longer, it was difficult to imagine any process that would make it shorter. The decisive clue came from Tucker who showed that hf phonons were all at $\omega \sim 10$ K [32] i.e. just above the energy where there is spontaneous phonon decay.

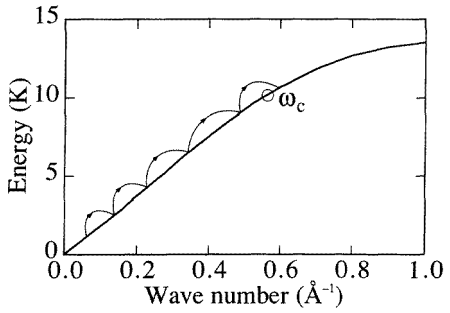

Figure 12. Schematic diagram of the chain of frequency up-conversion processes that creates a phonon with $\omega > \omega_c$.

The process of creating hf phonons starts with the heater injecting many low-frequency phonons into the liquid ^{4}He. Their density is high and they interact via the 3pp. Phonons of higher energy are created in the transient scattering region. There are fewer high-energy phonons for scattering but this is compensated by the 3pp which has a rapidly increasing scattering strength with energy. A small fraction of the phonons reach 8 K which is the maximum energy possible by 3pp. At this point a phonon with $\omega \sim 8$ K interacts with a low-energy phonon by the 4pp and if this creates a phonon with $\omega > 10$ K it is then relatively stable. It is indeed quite stable if it can propagate into a region of liquid where there are no low-energy phonons. It is these hf phonons that we detect. This model is shown schematically in figure 12. The up-scattering model explains why the hf phonons are just above ω_c. Also it naturally gives a faster phonon–atom signal as part of the path length in the liquid is covered by fast low-energy phonons. The measured times of flight can be explained if the hf phonons are created up to ~ 4 mm from the heater.

The model has been confirmed by measuring the time of flight, between a fixed heater and bolometer, as a function of liquid path length. The time of flight is a linear function of depth whereas the shortest time of flight, calculated for a spectrum of hf phonons propagating all the way from the heater, gives a longer time for similar path lengths for the phonon and atom. Furthermore the function is not linear as is shown in figure 13 [33]. There is no

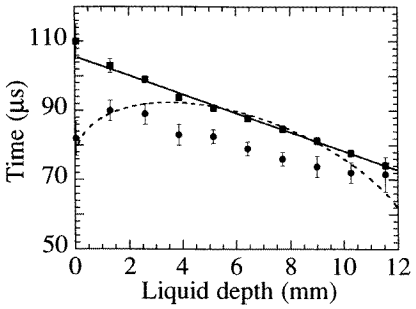

Figure 13. The circles show the fastest phonon–atom signals over a distance of 12 mm as a function of liquid path length. The dotted line is calculated on the basis of a spectrum of high-energy phonons created at the heater and is significantly slower. The squares show the times when the peak flux arrives and the solid line is calculated for 10.5 K phonons.

evidence that contradicts this model; however as yet there is no detailed theoretical study of this strongly interacting phonon gas.

7. Wetting studies using liquid ^{4}He

Wetting studies can of course be done with most liquids and there is no fundamental reason why it should be done with liquid ^{4}He. There are however compelling advantages in using liquid ^{4}He. The first is that the liquid ^{4}He–Cs combination shows a wetting transition (T_w) at 2 K which is an easily accessible temperature, and secondly it is possible to get thermodynamic equilibrium for the measurements. Wetting transitions are expected below the critical point [34, 35] but it appears that T_w is too close to the critical temperature to study it with other liquids.

Liquid He wets most materials; the exceptions are Cs and Rb and these elements with surface oxide layers. It was predicted by Cheng *et al* [36] that the alkali metals might not be wetted by liquid ^{4}He because the interaction potential between the ^{4}He and caesium is weaker than for ^{4}He–^{4}He, so the droplet state of ^{4}He has a lower energy than the liquid being spread out over the Cs. The ^{4}He–Cs interaction potential has a shallow minimum because of the large 6s orbital of the Cs which repels the ^{4}He and cuts off the van der Waals attractive force.

The theory of wetting and prewetting had developed for over a decade without any experimental input because of the lack of suitable systems. It was predicted that the wetting transition could be first- or second-order and if it was first-order then there should be prewetting [37, 38]. Prewetting is a surface phase change where the order parameter is the thickness of the film of liquid on the solid surface. At each point on the prewetting line, two distinct film thicknesses coexist.

Cs was first shown to be not wetted by liquid ^{4}He by Nacher and Dupont-Roc [39]. The wetting temperature and prewetting behaviour was found by Rutledge and Taborek [40] using a quartz oscillator microbalance to detect thin–thick-film transition. Cs was shown to be essentially free of any adsorbed ^{4}He at $T \ll T_w$ by Stefanyi *et al* [41].

If a liquid only partially wets a substrate then there is a finite contact angle between the surface of the bulk liquid and the substrate. As the wetting temperature is approached from below, the contact angle decreases and goes to zero at T_w with an asymptotically infinite gradient.

The contact angle for ^{4}He on Cs was found by measuring the force on the liquid due to a set of parallel plates dipping into the free surface. The plates were tungsten coated with Cs and the pressure in the liquid was measured with a capacitance gauge. The results are shown in figure 14 [42]. They show in a direct way the reality of the wetting transition.

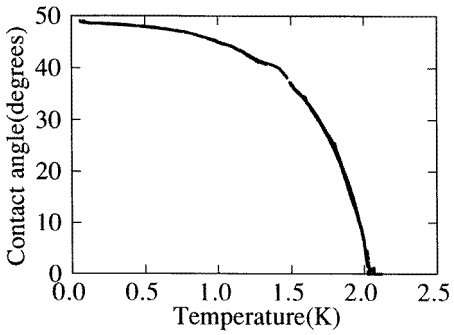

Figure 14. The contact angle between ^{4}He and Cs as a function of temperature.

From the measurements of the contact angle and the measured surface tension of liquid ^{4}He, the surface free energy of the liquid ^{4}He–Cs interface can be obtained. This shows a temperature dependence which is similar to that of the surface tension. This suggests that there are ripplons at this interface as well as on the free surface [43]. This is a surprising result as it was thought that ripplons would be suppressed by the incompressible Cs surface.

8. Conclusions

This review has not attempted to cover all the latest work on liquid ^{4}He. So I have omitted the neutron scattering studies on bulk liquid and thin films, the Kosterlitz–Thouless transition and torsional oscillator studies, the Josephson effect and the creation of vortices, the propagation of ions and the ions and electrons at the surface of liquid ^{4}He, and liquid ^{4}He in confined geometries. Nor have I included a discussion of the theoretical developments which continue apace. Instead I have concentrated on quantum evaporation and wetting which illustrate the two parts of the title that liquid ^{4}He is extraordinary in that the elementary excitation are long lived and can be studied in some detail, and that liquid ^{4}He is an ordinary liquid for wetting experiments which confirm many of the theoretical predictions about the nature of the surface phase transition.

Acknowledgments

I am indebted to many colleagues with whom I have had the pleasure of working with over recent years. These include M Brown, A C Forbes, M A H Tucker, C D H Williams, P Stefanyi and J Klier.

References

[1] Palevsky H, Otnes K and Larsson K E 1958 *Phys. Rev.* **112** 11–18
Yarnell J L, Arnold G P, Beadt P J and Kerr E C 1959 *Phys. Rev.* **113** 1379–86
Henshaw D G and Woods A D B 1961 *Phys. Rev.* **121** 1266–74

Stirling W G 1983 *75th Jubilee Conf. on Helium-4* ed J G M Armitage (Singapore: World Scientific) p 109; 1991 *Excitations in Two-Dimensional and Three-Dimensional Quantum Fluids* ed A F G Wyatt and H J Lauter (New York: Plenum Press) p 25
[2] Feynman R P 1953 *Phys. Rev.* **91** 1301; 1954 *Phys. Rev.* **94** 264
[3] Pitaevskii L P 1992 *J. Low Temp. Phys.* **87** 127
[4] Galli D E, Reatto L and Vitiello S A 1995 *J. Low Temp. Phys.* **101** 755
[5] Miller A, Pines D and Nozières P 1962 *Phys. Rev.* **127** 1452
[6] Maris H J and Massey W E 1970 *Phys. Rev. Lett.* **25** 220
[7] Mills N G, Sherlock R A and Wyatt A F G 1975 *J. Phys. C: Solid State Phys.* **8** 2575
[8] Slukin T J and Bowley R M 1974 *J. Phys. C: Solid State Phys.* **7** 1779–85
[9] Jackle J and Kehr K W 1971 *Phys. Rev.* **27** 654
[10] Dynes R C and Narayanamurti V 1974 *Phys. Rev. Lett.* **33** 1195
[11] Wyatt A F G, Lockerbie N A and Sherlock R A 1974 *Phys. Rev. Lett.* **33** 1425–8
[12] Pitaevskii L P 1959 *Sov. Phys.–JETP* **36** 830
[13] Brown M and Wyatt A F G 1990 *J. Phys.: Condens. Matter* **2** 5025–46
[14] Sears V F, Svensson E C, Martel P and Woods A D V 1982 *Phys. Rev. Lett.* **49** 279
[15] Baddar H, Edwards D, Levin T M and Pettersen M S 1995 *Workshop on Quantum Evaporation, Condensation and Sticking Phenomena* (Pisa, 1995)
[16] Brown M and Wyatt A F G to be published
[17] Wyatt A F G, Tucker M A H and Cregan R 1995 *Phys. Rev. Lett.* **74** 5236
[18] Mulheran P A and Inkson J C 1992 *Phys. Rev.* B **46** 5454
[19] Dalfovo F, Frachetti A, Lastri A, Pitaevskii L and Stringari 1995 *Phys. Rev. Lett.* **75** 2510
[20] Dalfovo F, Frachetti A, Lastri A, Pitaevskii L and Stringari 1996 *J. Low Temp. Phys.* at press
[21] Tucker M A H and Wyatt A F G 1996 *Czech. J. Phys.* **46** S1 263
[22] Tucker M A H and Wyatt A F G 1992 *J. Phys.: Condens. Matter* **4** 7745–58
[23] Tucker M A H and Wyatt A F G unpublished
[24] Landau L D and Khalatnikov I M 1949 *Sov. Phys.–JETP* **19** 637–50
[25] Wyatt A F G 1993 *Phys. Scr.* T **49** 59–64
[26] Mezei F 1980 *Phys. Rev. Lett.* **44** 1601
[27] Forbes A C and Wyatt A F G 1990 *Phys. Rev. Lett.* **64** 1393–6
[28] Wyatt A F G and Forbes A C 1991 *Excitations in Two-Dimensional and Three-Dimensional Quantum Fluids* ed A F G Wyatt and H J Lauter (New York: Plenum) p 137
[29] Iwamoto F 1991 *Excitations in Two-Dimensional and Three-Dimensional Quantum Fluids* ed A F G Wyatt and H J Lauter (New York: Plenum) p 149
[30] Pitaevskii L P 1991 *Phys. Lett.* **153A** 478
[31] Forbes A C and Wyatt A F G 1990 *Physica* B **165 & 166** 497
[32] Tucker M A H and Wyatt A F G 1994 *J. Phys.: Condens. Matter* **6** 2813–24
[33] Forbes A C and Wyatt A F G to be published
[34] Cahn J W 1977 *J. Chem. Phys.* **66** 3667
[35] Ebner C and Saam W F 1977 *Phys. Rev. Lett.* **38** 1486
[36] Cheng E, Cole M W, Saam W F and Treiner J 1991 *Phys. Rev. Lett.* **67** 1007; 1992 *Phys. Rev.* B **46** 13 967
[37] Schick M 1990 *Liquids at Interfaces* ed J Charvolin, J E Joanny and J Zinn-Justin (Amsterdam: Elsevier) p 415–97
[38] Dietrich S 1987 *Phase Transitions and Critical Phenomena* vol 12, ed C Domb and J L Lebowitz (New York: Academic)
[39] Nacher P J and Dupont-Roc J 1991 *Phys. Rev. Lett.* **67** 2966
[40] Rutledge J E and Taborek P 1992 *Phys. Rev. Lett.* **69** 937; 1993 *Phys. Rev. Lett.* **71** 263
[41] Stefanyi P, Klier J and Wyatt A F G 1994 *Phys. Rev. Lett.* **73** 692
[42] Klier J, Stefanyi P and Wyatt A F G 1995 *Phys. Rev. Lett.* **75** 3709
[43] Klier J and Wyatt A F G 1996 *Czech. J. Phys.* **46 S1** 439